

Effect of Temperature, CO₂ Pressure, and Brine Composition on the Layer Spacing of Montmorillonite

BY

Jacqueline Kowalik
B.S., Winona State University, 2008

THESIS

Submitted as partial fulfillment of the requirements
for the degree of Masters of Science in Earth and Environmental Sciences
in the Graduate College of the
University of Illinois at Chicago, 2021

Chicago, Illinois

Defense Committee:

Stephen Guggenheim, Chair and Advisor
August Koster van Groos, Department of Earth and Environmental Sciences
D'Arcy Meyer-Dombard, Department of Earth and Environmental Sciences

I dedicate this work to my son, Orion, who has inspired me to push beyond my limits and accomplish things I did not think were possible.

ACKNOWLEDGEMENTS

I would like to thank my committee members, not only for their help and support, but also for their time and patience as I completed my Master's in a slightly longer than anticipated time frame. I would like to extend my deepest gratitude to my graduate advisor, Steve Guggenheim, and to A.F. Koster van Groos, who are the reason my research was made possible, as well as Paolo Benavides, who has helped me significantly over the last year as I pushed to complete my thesis. I would also like to thank my friends and family, those closest to me, that have kept me moving forward through all of this.

CONTRIBUTION OF AUTHORS

Summary represents a published abstract [Kowalik, J., Guggenheim, S., Koster van Groos, A.F. (2015, July 5-10). Effects of temperature, pressure, and brine composition on the interlayer spacing of montmorillonite at *in situ* conditions using CO₂. Euroclay 2015, Edinburgh, Scotland.] for which I was the primary author and major driver of the research. Thesis Body represents a published manuscript (Benavides, P.A., Kowalik, J., Guggenheim, S., Koster van Groos, A.F., 2020. Effect of CO₂ pressure, temperature, and brine composition on the interlayer spacing of Na-Rich and K-exchanged montmorillonite. Applied Clay Science 198.) for which I was the second author. I played a large role in the introductory and exploratory research, investigation, and experimentation, which was used and re-examined by the first author, Paolo Benavides.

TABLE OF CONTENTS

1. INTRODUCTION	1
2. PREVIOUS WORK.....	3
3. METHODS.....	6
3.1 Equipment	6
3.2 Sample Preparation.....	6
3.3 Experimental Conditions	7
3.4 Data Collection	8
3.5 Data Correction	8
4. RESULTS.....	10
4.1 Diffraction.....	10
4.2 Experiments with $P(\text{CO}_2)$ and with $P(\text{He})$ to ~500 bars and T at ~31°C.....	11
4.3 Experiments with initial $P(\text{CO}_2)$ and $P(\text{He})$ at ~ 500 bars and increasing T from ~31° to 150°C	16
5. DISCUSSION AND CONCLUSION	20
REFERENCES	23
APPENDIX	26
VITA	27

LIST OF TABLES

<u>TABLE</u>		<u>PAGE</u>
I.	BRINE SOLUTION COMPOSITIONS	7
II.	X-RAY DATA COLLECTION PARAMETERS.....	8
III.	CARBON DIOXIDE PRESSURE DATA.....	12
IV.	HELIUM PRESSURE DATA	15
V.	CARBON DIOXIDE TEMPERATURE DATA.....	17
VI.	HELIUM TEMPERATURE DATA	18

LIST OF FIGURES

<u>FIGURE</u>	<u>PAGE</u>
1. Representative diffraction pattern for montmorillonite (Na-SWy2) clay in NaCl Brine.....	11
2. Effect of brine composition on the $d(001)$ at near ambient conditions	13
3. Effect of NaCl brine compositions and $P(\text{CO}_2)$ on the $d(001)$ of montmorillonite (Na-SWy2) clay at near ambient temperatures.....	14
4. Comparison of the effects of Helium versus CO_2 gas pressure on the $d(001)$ of montmorillonite (Na-SWy2) clay at near ambient temperatures.....	15
5. Effect of NaCl brine composition and temperature at starting $P(\text{CO}_2) \approx 500$ bars on the $d(001)$ of montmorillonite (Na-SWy2) clay.....	18
6. Comparison of the effects of Helium versus CO_2 gas pressures starting at ~ 500 bars and increasing temperature on the $d(001)$ of montmorillonite (Na-SWy2) clay	19

LIST OF ABBREVIATIONS

CO ₂	carbon dioxide
Na	sodium
NaCl	sodium chloride
He	helium
Ca	calcium
Mg	magnesium
K	potassium
H ₂ O	water molecule
Mo	molybdenum
<i>T</i>	temperature
<i>P</i>	pressure
<i>P</i> (CO ₂)	pressure using carbon dioxide as the pressurizing gas
<i>P</i> (He)	pressure using helium as the pressurizing gas
<i>P</i> (H ₂ O)	pressure using water as a pressurizing gas
<i>a</i> (H ₂ O)	activity of water
ScCO ₂	supercritical carbon dioxide
<i>d</i> (001)	perpendicular distance between parallel planes as represented by the (001) Miller index
<i>d</i> (003)	perpendicular distance between parallel planes as represented by the (003) Miller index
<i>d</i> (005)	perpendicular distance between parallel planes as represented by the (005) Miller index
°C	degrees Celsius
M	molar
m	molal
Å	Angstrom
mL	milliliters

kV	kilovolt
mA	milliamp
mm	millimeters
cm	centimeters
g/L	grams per liter
g	grams
ppm	parts per million
wt %	weight percent
kbar	kilobars
MD	molecular dynamic
HPEC	high-pressure environmental chamber
O.D.	outer diameter

SUMMARY

[Previously published as Kowalik, J., Guggenheim, S., Koster van Groos, A.F. (2015, July 5-10). Effects of temperature, pressure, and brine composition on the interlayer spacing of montmorillonite at *in situ* conditions using CO₂. Euroclay 2015, Edinburgh, Scotland.]

The effect of CO₂ on a Na-rich montmorillonite smectite (Clay Minerals Society Source Clay, SWy-2), a common clay mineral found in fine-grain, clastic sedimentary rocks, was examined as a function of temperature (T), pressure using CO₂ gas [$P(\text{CO}_2)$], and NaCl brine composition. For comparison, the clay mineral was investigated at the same conditions, but in the presence of He [$P(\text{He})$]. The molar volume of SWy-2, as determined by the direct measurement of $d(001)$, was determined using X-ray diffraction techniques and a specially constructed environmental chamber. Measurements were made at $P(\text{CO}_2)$ and $P(\text{He})$ to ~1000 bars and temperatures to 150°C, with eight NaCl brine compositions ranging from 0.17 M to NaCl saturation. These conditions include the environment where CO₂ sequestration in deep-seated sedimentary rocks is being considered for entrapment.

At $P(\text{CO}_2) = 1$ bar and $T \sim 31^\circ \text{C}$, a change in brine composition from 0.17 M to 5.99 M resulted in $d(001)$ decreasing from 22.6 Å to 16.7 Å (26%). Increasing $P(\text{CO}_2)$ from 1 to 500 bars at $T \sim 31^\circ \text{C}$ resulted in a decrease in $d(001)$, with increasing pressures having greater effects on lower salinity brines. With increasing pressure to $P(\text{CO}_2) = 500$ bars at $T \sim 31^\circ \text{C}$ and in 0.68 M brine, $d(001)$ decreased from 19.7 Å to 19.0 Å (4%). Increasing T from ~31 to 150°C at an initial $P(\text{CO}_2) = 500$ bars resulted in a decrease in $d(001)$ with temperature having greater effects on lower salinity brines. With increasing T from ~31 to 150°C, $d(001)$ values of montmorillonite in 0.17 M brine decreased from 19.6 Å to 19.0 Å (3%), whereas $d(001)$ in 5.99 M brine did not significantly change. The greatest decrease in $d(001)$ with increasing T at initial $P(\text{CO}_2) = 500$ bars occurred for brine compositions of 1.37 M and 1.71 M. For the T interval from

100 to 150°C, $d(001)$ decreased from 19.0 Å to 17.2 Å (10 %) for clay in the 1.37 M NaCl brine. In a 1.71 M NaCl brine and with an increase from $T = 50$ to 150°C, $d(001)$ decreased by 16% (18.6 to 15.7 Å). Results with $P(\text{He})$ to ~500 bars and increasing T to 150°C using 1.37 M and 3.42 M brines were identical, within error, to the CO_2 results.

Results show the importance of the activity of water ($a_{\text{H}_2\text{O}}$) and temperature on the interlayer H_2O content, especially brine concentration, whereas pressure is of less importance. Because the results of the He experiments and the CO_2 experiments were essentially identical, it is concluded that CO_2 does not enter into the clay interlayer under these experimental conditions. The loss of interlayer H_2O would result in a large decrease in molar volume with increasing temperature (up to ~16%) and may result in dehydration cracking within the CO_2 -confining shales associated with CO_2 -sequestration reservoirs. Additionally, changes in molar volume could negatively impact the permeability and porosity of the reservoir rock. Thus, the brine concentration is an important parameter to consider before CO_2 injection.

(Previously published, in part, as Benavides, P.A., Kowalik, J., Guggenheim, S., Koster van Groos, A.F., 2020. Effect of CO₂ pressure, temperature, and brine composition on the interlayer spacing of Na-Rich and K-exchanged montmorillonite. *Applied Clay Science* 198.)

1. INTRODUCTION

Sequestering carbon dioxide (CO₂) in deep sedimentary rock has been proposed by numerous authors as a viable method to lessen the increase of anthropogenic CO₂ in the atmosphere (e.g., IPCC, 2005). CO₂ is to be pumped and stored in a reservoir as supercritical CO₂ (scCO₂) that is sealed by an impermeable cap rock formation (“hydrodynamic” trapping), where the CO₂ displaces a brine. Whereas most of the CO₂ will not react with the existing phases in this environment, some CO₂ will dissolve in a brine or petroleum (“solubility” trapping) or react with some mineral phase to form carbonate (“mineral” trapping) or an adsorbate (or solvate) in a clay mineral. Lin et al. (2008) postulates that four different “reaction systems” may be associated with the scCO₂ injection: (1) a dry CO₂–rock reaction near the injection site, (2) a CO₂–brine–rock reaction system adjacent to the CO₂ injection, (3) a CO₂–brine–rock reaction system near the edge of the injection field, and (4) a brine–rock reaction system involving the displaced brine. The temperature and pressure at CO₂ injection sites are commonly greater than 30°C and 100 bars, respectively (Michael et al., 2010).

Sedimentary rocks for sequestration purposes are selected on their porosity and permeability, but an important condition is that these rocks are confined by sedimentary strata, such as clay-rich shales, with very low permeability to prevent CO₂ leakage from the system. Typical sedimentary rock formations suitable for CO₂ storage are, therefore, sandstone-shale sequences. Selection of a suitable rock formation requires detailed information on its porosity and permeability, its mineralogical composition including the clay mineral content, and its texture.

Smectite, known as a swelling clay for its capacity to absorb (or release) H₂O and other volatile components at the interlayer site, is commonly found in shales, and at lesser amounts in sandstones. In shales, smectite is most commonly present as interstratified (“mixed layers”) of illite/smectite [up to 62 weight % (wt %) of bulk mineralogy] and less commonly as smectite (up to 9 wt % of bulk mineralogy) (Espinoza and Santamarina, 2012). In sandstones, illite/smectite can comprise up to 5 wt % of the bulk mineralogy (Xu et al., 2003). The molar volume of these clay minerals, specifically smectites, can vary as a function of brine chemistry, temperature, and pressure, all of which are related to the activity of water in these rocks. Changes in water activity have the potential to decrease storage capacities of the sandstone reservoirs and/or increase permeability of shale caprocks.

In the present study, the reaction of montmorillonite, which is the most common smectite clay mineral, with CO₂ is examined because of the ubiquitous presence of this clay in reservoir and/or cap rocks. This study includes the effects of CO₂ and temperature, pressure, and brine composition on the molar volume of a montmorillonite. The reaction system consistent with this study is equivalent to the edges of the injection field (system 2), adjacent to the injection field (system 3) and beyond the injection field where water becomes dominant over CO₂ (system 4). In addition to understanding CO₂ interactions with montmorillonite, the implications of the present study suggest the need for an understanding of the long-term interactions that influence the behavior of montmorillonite in aqueous solutions, such as a brine. For comparison, more specifically to isolate the interaction of CO₂ with the interlayer, a parallel study is presented using Helium (He) instead of CO₂. He is an inert gas that is not expected to interact with the interlayer of montmorillonite, and as such, allows for the effect of CO₂ on the interlayer to be studied. An updated version of the present thesis has been published, in part, in Benavides et al. (2020).

2. PREVIOUS WORK

In the early 1950s, salinity was demonstrated to affect the layer-to-layer spacing [= $d(001)$] of montmorillonite clay (Norrish, 1954), using X-ray diffraction of the clay in the presence of various brines. Increasing the NaCl molarity of the brine resulted in the dehydration of montmorillonite, significantly decreasing molar volume (e.g., Norrish and Quirk, 1954; Slade et al., 1991). Colten (1986) used a high-pressure (hydraulic pressure application) X-ray environmental chamber to determine $d(003)$ and $d(005)$ of Na-exchanged montmorillonite (Cheto, AZ, SAz-1) in 1 and 5 molal NaCl solutions at 34.5 and 152 bars (1m) and 52 and 462 bars (5m). The change in $d(001)$ of montmorillonite (Ca- and Mg-exchanged montmorillonite, SWy-1, in pure H₂O, Wu et al., 1997; Na-exchanged SWy-1, Huang et al., 1994) at very high (<13 kbar) pressure was directly observed in diamond anvil cells, but simulating the conditions of sedimentary basins proved to be difficult with these cells (Guggenheim and Koster van Groos, 2014).

In more recent experiments, clay molar volume changes [i.e., $d(001)$] are studied indirectly because of the experimental difficulties in measuring $d(001)$ by X-ray diffraction: 1) X-ray dispersion from the brine decreases the overall intensity of the X-ray incident beam and increases background, 2) reactions between clays and aqueous fluids are rapid and non-quenchable, and 3) clays flocculate (coagulate) and do not remain in suspension in brines. Most recent studies theoretically model the effect of salinity on clay (e.g., Underwood et al., 2015; Omekeh et al., 2004) or monitor parameters (e.g., flow, permeability; Morsy and Sheng, 2014; Xu et al., 2014) that are believed to be influenced by clay molar volume. However, although the clay-particle molar volume may partly explain the results of these indirect studies, there are other variables to consider, such as pore-throat shape, size and connectivity, or variations in clay compaction, orientation, and chemical composition, or variations in wettability.

To address clay molar volume directly by experiment using X-rays, a prototype X-ray cell was used to study CO₂ interactions with Na-rich montmorillonite smectite under limited (nearly dry) reservoir conditions (Giesting et al., 2012a; 2012b). Both Giesting et al. and Loring et al. (2013), the latter using a cell of a different design, but with similar limitations, found that when the smectite interlayer contained zero to one plane of H₂O molecules, CO₂ can be adsorbed within the interlayer. By using variably hydrated scCO₂, Schaef et al. (2015) showed that CO₂ does not enter the interlayer when it is dehydrated or when it contains more than one H₂O plane in Na-, Ca-, or Mg-exchanged montmorillonite. Simulations supported these results and provided insight to the CO₂ + H₂O interactions. For example, molecular dynamic (MD) simulations (Sena et al., 2015) of CO₂ and Na-rich montmorillonite-H₂O interfaces showed that H₂O and CO₂ cluster in a central single plane in the interlayer. The Na clusters separately with H₂O. CO₂ clusters, segregated from H₂O, form by CO₂ – CO₂ interactions. Na is capable of migrating via the clusters of H₂O across the central plane. Free energy curves calculated by multiphase Monte Carlo and MD simulations for Na in the interlayer of beidellite and montmorillonite show that the beidellite has a single plane of CO₂ + H₂O whereas the montmorillonite has both a monoplanar and a biplanar configuration (Makaremi et al., 2015). These adsorbate reactions involving H₂O and CO₂ are best described as occurring in the “reaction system” of Lin et al. (2008) where there is a near water-free supercritical CO₂ environment at or near the injection site.

These studies establish the importance of the initial hydration state (interlayer H₂O content), but the studies did not fully determine the separate effects of temperature (T), pressure [$P(\text{CO}_2)$], activity of water [$a(\text{H}_2\text{O})$], and brine composition on the interlayer H₂O content of smectites either at the injection site or, and especially, at water-saturated conditions further from the injection site. To obtain these data, a high-pressure environmental chamber (HPEC) was developed to study real-time

experiments to 1000 bars pressure and 150°C in aqueous fluids (Guggenheim and Koster van Groos, 2014). The HPEC is unique because it allows the sample and liquid (~2 mL) to form a dynamic system, where particles can move freely in the liquid while being illuminated by the X-ray beam. Thus, clay minerals may be studied in a steady state environment with a coexisting liquid and pressurizing gas at elevated pressures and temperatures, regardless whether flocculation of the clay occurs.

3. EXPERIMENTAL METHOD

3.1 Equipment

Experiments were conducted using a high-pressure environmental chamber (HPEC, Guggenheim and Koster van Groos, 2014) made from a titanium alloy (Ti-6Al-4V ELI, ASTM grade 5). The chamber allows pressures to 1000 bars and temperatures to 150°C. The HPEC was mounted on a transmission-mode Bruker D8 three-circle diffractometer, with Mo (0.7107 Å) radiation, operating at 45 kV and 25 mA. The diffractometer was equipped with a 0.3° divergence Monocap collimator, an incident-beam graphite monochromator, and an APEX CCD area detector (1024 x 1024 pixels) at a distance of 120 mm from the center of the clay-brine sample. Data frames were collected at $2\theta = 0^\circ$ (allowing $d \approx 27.1$ Å) for 20 minutes (1200 seconds) using Bruker SMART (v. 5.6.635, 2010) software. The HPEC was pressurized by CO₂ or He gas. Pressures were measured using a calibrated Heise gauge or an in-line pressure transducer, both believed accurate to within 1%. Six cartridge heaters (3.3 mm O.D., 2.5 cm long) inserted in holes near the top (3) and the bottom (3) of the HPEC allowed the chamber to be heated. Temperatures were measured using a K-type thermocouple located within 2 mm of the irradiated sample. In experiments where external heaters were not used, heat produced by the internal pump of the HPEC raised the temperature to 31 to 33°C.

3.2 Sample Preparation

Na-rich montmorillonite clay (Clay Minerals Society Source Clay SWy-2, Costanza and Guggenheim, 2001 and papers therein) was used as-received. Eight brine solutions were prepared (Table I) using Fisher Chemicals NaCl (Lot No. 052761, ACS grade).

Table I. Brine solution compositions

NaCl Content (g/L)	Molarity (M)
10	0.17
20	0.34
40	0.68
80	1.37
100	1.71
120	2.05
200	3.42
>350	>5.99

3.3 Experimental Conditions

Approximately 0.2 g of SWy-2 sample (0.4 g for brines > 3.42 M) was loaded into the HPEC together with approximately 2 mL of brine solution. Preliminary X-ray data were collected at ambient pressure and temperature (approximately 1 bar in air without additional CO₂, and approximately 31°C). Next, pressure was increased stepwise from ambient to approximately 500 bars using either CO₂ (Air Gas, <10 ppm H₂O) or He (Prosier, high purity, grade 5) gas as a pressure medium. X-ray data were collected with pressures from approximately 0, 20-30, 50-60, 100, 200, 300, 400, to 500 bars (with $T \sim 31^\circ\text{C}$). After X-ray data were collected at 500 bars and approximately 31°C, the HPEC was sealed from the pressure-intensifier unit to prevent loss of material during heating. Next, the temperature of the HPEC was increased stepwise to $T = 50^\circ, 75^\circ, 100^\circ, 125^\circ$, and 150°C (with P initially set at approximately 500 bars, but increasing with increasing temperature). At each step, the temperature was maintained constant for 30 minutes to allow the system to reach equilibrium, after which X-ray data were collected. A 30-minute equilibration period was considered sufficient, because preliminary data indicated that a steady state equilibrium was reached within 20 minutes. X-ray data collection parameters are summarized in Table II.

Table II. X-ray data collection parameters.

X-ray Image	T (°C)	P (bars)
1	~28-32	0
2		20-30
3		50-60
4		100
5		200
6		300
7		400
8		500
9	50	~500
10	75	~600
11	100	~750
12	125	~875
13	150	~1000

3.4 Data Collection

An internal magnetic-controlled pump circulates the sample within the HPEC and allows the clay particles to move freely in the liquid, thus establishing a suspension of clay in the brine and maintaining a steady-state condition during data collection. X-ray data were collected as the clay particles and brine passed between two parallel 1-mm thick diamond windows. Images were processed using the Bruker application GADDS (v. 4.1.14, 2003) software before importing into Materials Data, Inc. JADE+ (v. 9.4, 2011) software to obtain peak positions and full-width at half-maximum values. The APEX data were calibrated to the GADDS software using chlorite with a known (001) diffraction peak of 14.2 Å.

3.5 Data Corrections

Early experiments involved pressure determination using an inline pressure transducer mounted near the external pump. This limited accurate recording of pressure conditions at the pump when the HPEC operated as an open system. Later experiments involved a pressure

transducer mounted at the HPEC to accurately record pressure during closed-system tests. For the 500 bar experiments, the HPEC was filled with a brine solution and pressure was increased to $P=500$ bars. The HPEC was sealed and heated incrementally from $T\sim 31^{\circ}\text{C}$ to $T=150^{\circ}\text{C}$. Pressure was recorded at $T= 50^{\circ}, 75^{\circ}, 100^{\circ}, 125^{\circ}$, and 150° C. Pressure data was plotted and a best fit line equation calculated (Equation 1), where P is pressure and T is temperature. Previously collected pressure data was corrected based on this equation.

$$P = 5.1169T + 364.4 \quad (1)$$

4. RESULTS

4.1 Diffraction

A representative diffraction pattern for montmorillonite (Na-SWy2) clay in a 1.71M NaCl brine at $P(\text{CO}_2) = 220$ bars and 33.7°C is shown in Figure 1. Clay-peak intensities are high and background is relatively low, and no background subtraction involving clay-free brine is required (Guggenheim and Koster van Groos, 2014). The relatively broad $d(001)$ peak, shown by the lower bar at approximately 1 to 3 $^\circ 2\theta$ results from the average of multiple hydration states in the clay sample; these represent random interstratification of many layer-to-layer spacings. From the width of the upper bar, labeled $2\theta_1 - 2\theta_2$ and located at $\frac{1}{2}$ of the peak height, the 2θ value of $d(001)$ of the average layer-to-layer spacing of the sample is determined (Tables III – VI, Figures 2 – 6). Because the $d(001)$ peak is at low 2θ angles, the errors associated with the peak values are expected to be high ($\pm 0.2^\circ$). The higher-order peaks (i.e., at 2θ values of 9.4° and 12.5°) are non-integral diffraction peaks and cannot be properly indexed. These very broad, asymmetrical peaks (“ hk bands”) result from the lack of a truly periodic diffraction condition required by the derivation of the Bragg equation.

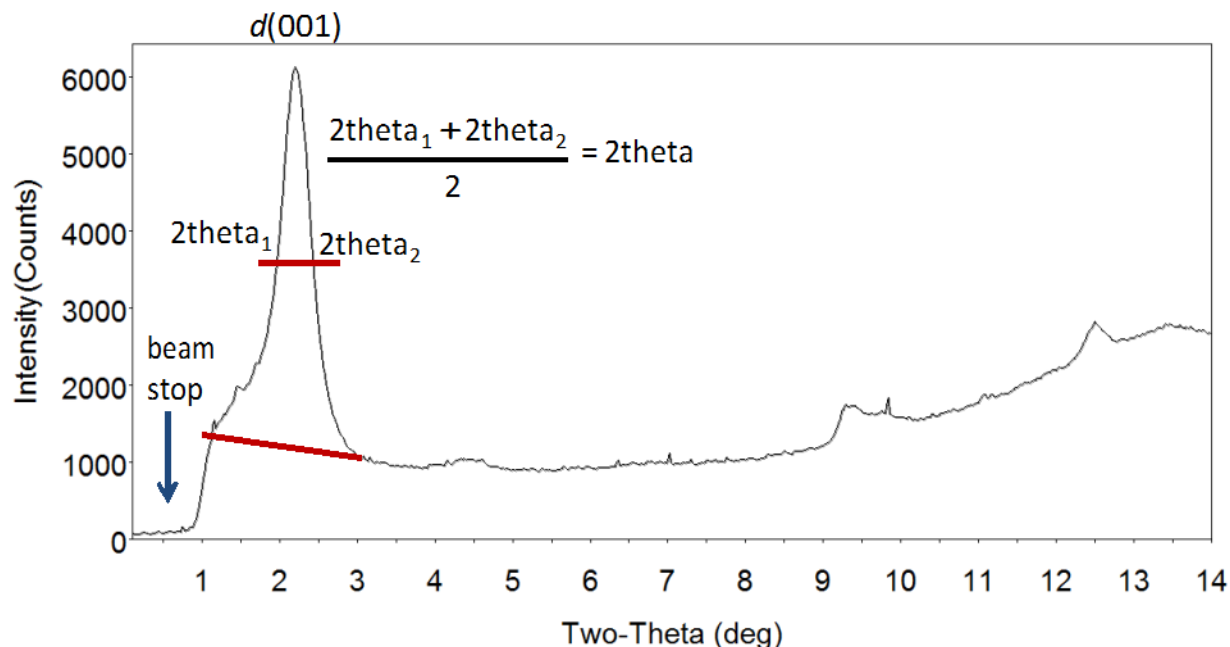


Figure 1. Illustration of a diffraction pattern taken at $P(\text{CO}_2) = 221.6$ bars, $T = 33.7^\circ \text{C}$, NaCl brine = 1.71 M, with determination of $d(001)$ of $\sim 18.6 \text{ \AA}$. The broad peaks at 2θ of $\sim 9.4^\circ$ and $\sim 12.5^\circ$ are diffraction bands. The arrow at 2θ of $<1^\circ$ shows the effect of the beam stop. No radiation.

4.2 Experiments with $P(\text{CO}_2)$ and with $P(\text{He})$ to ~ 500 bars and T at $\sim 31^\circ \text{C}$

The results of experiments with eight brine compositions (0.17M, 0.34M, 0.68M, 1.37M, 1.71M, 2.05M, 3.42M, $>5.99\text{M}$) are listed in Table III and shown in Figures 2, 3, and 4. At ambient pressure and temperature (i.e. no added CO_2 and approximately 31°Celsius) the $d(001)$ values of Na-SWy2 in these brine compositions decrease with increasing salinity (Table 3, Figure 2). These results are consistent with earlier clay-brine studies (Norrish, 1954 and Slade et al., 1991), with differences in the results potentially reflecting the different montmorillonite used between the studies and that the current study involves free floating clay suspensions, allowing the clay samples to reach equilibrium with the brine solution. The sharp decrease in $d(001)$ values (18.9 \AA to 16.6 \AA to 15.7 \AA) at brine compositions of 1.71M to 2.05M to 3.42 M (Figure 2) represents a decrease of the interlayer H_2O content.

Table III. Values of $d(001)$ for Na-SWy2 with $P(\text{CO}_2)$ to ~500 bars and temperatures from ~27 to ~34°C

M	$P(\text{CO}_2)$ (bar)	T (°C)	$d(001)$ (Å)	M	$P(\text{CO}_2)$ (bar)	T (°C)	$d(001)$ (Å)
0.17	0	27.0	---	1.71	0	30.0	18.9
	27.2	31.4	---		31.1	32.1	18.7
	55.6	32.7	20.4		56.0	33.1	18.7
	114.5	33.2	20.2		121.1	33.5	18.7
	220.9	33.6	19.9		221.6	33.7	18.6
	314.8	33.6	19.9		321.5	33.9	18.6
	411.7	33.8	19.9		398.3	33.4	18.6
	508	32.6	19.6		505.1	33.6	18.6
0.34	0	26.7	---	2.05	0	29.7	16.6
	26.5	30.8	---		26.3	31.4	16.6
	55.5	32.2	20.3		56.6	32.0	16.5
	114.3	32.8	20.2		107.7	32.3	16.5
	215.2	33.8	20.2		213.3	32.4	16.5
	319.1	33.4	20.0		326.1	32.5	16.4
	416.1	33.5	19.4		419.5	32.5	16.4
	514.7	---	---		513.5	32.6	16.3
0.68	0	29.5	19.7	3.42 ^a	0	31.2	15.9
	18.1	32.3	19.5		27.6	32.4	15.9
	45.2	32.9	19.5		57.6	33.0	15.8
	104.6	33.1	19.5		114.3	33.0	15.8
	203.0	33.3	19.5		214.9	33.1	15.8
	319.2	33.0	19.2		317.8	33.1	15.8
	405.3	32.9	19.0		412.7	33.2	15.8
	490.1	33.0	19.0		508.8	33.3	15.8
1.37 ^a	0	30.2	19.3	>5.99	0	30.2	15.7
	27.2	31.7	19.3		34.6	32.2	15.7
	54.2	32.4	19.2		54.3	32.8	15.7
	116.6	32.9	19.2		121.0	33.1	15.7
	218.7	32.2	19.2		212.7	33.3	15.7
	308.5	31.8	19.0		313.9	33.4	15.7
	415.6	33.1	19.1		403.4	32.9	15.5
	506.2	33.2	19.0		495.8	32.9	15.5

^a Values represent averaged data from three series. Errors in $d(001)$ values believed to be $\pm 2.5\%$

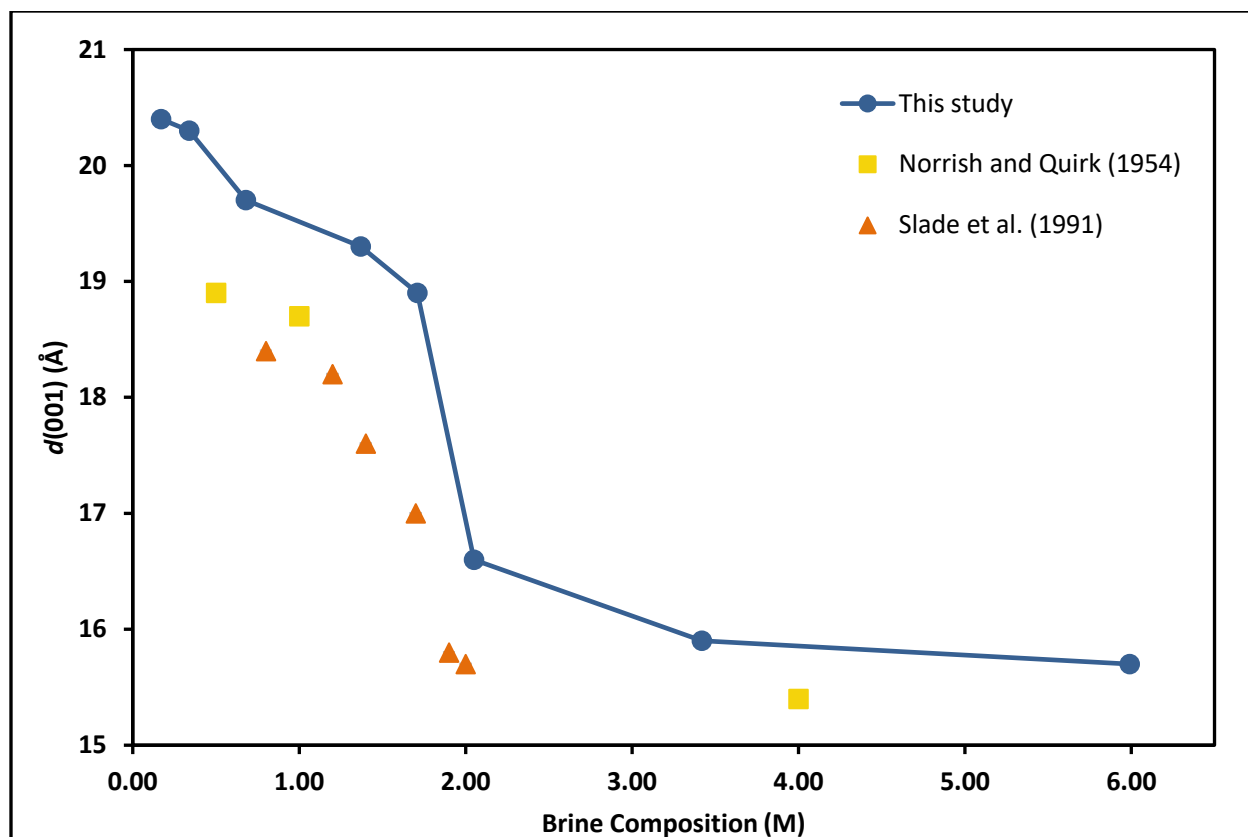


Figure 2. Effect of brine compositions on $d(001)$ at near ambient conditions (circles, this study; triangles, Norrish, 1954; boxes, Slade et al., 1991). The $d(001)$ standard errors are believed to be ± 0.2 Å.

Because the Na content of the interlayer is a consequence of the layer charge of montmorillonite, Na – Na interactions become important as the layer-to-layer distance decreases with interlayer H₂O loss with increasing salinity. These cation-to-cation interactions probably affect the H₂O configurations around the Na, and thus affects shielding. Figure 3 shows $d(001)$ versus $P(\text{CO}_2)$ to ~500 bars at $T \sim 31^\circ\text{C}$. Standard errors for pressure are not shown. The results at higher pressures are very similar to the experiments at $P(\text{CO}_2) = 1$ bar. With increasing $P(\text{CO}_2)$, $d(001)$ decreases by 1 – 4%, with increasing pressures having greater effects on lower salinity brines.

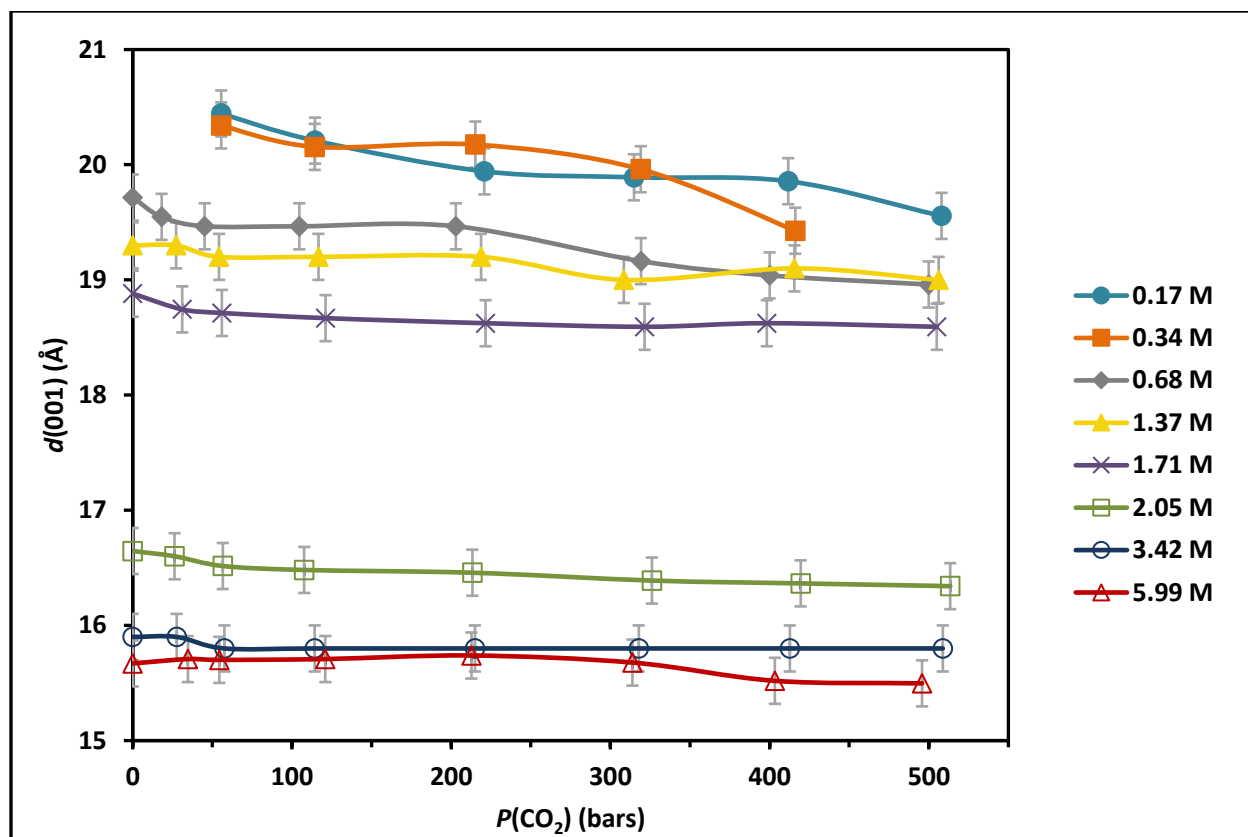


Figure 3. Effect of NaCl brine compositions and $P(\text{CO}_2)$ on the $d(001)$ of montmorillonite at $T \sim 31^\circ\text{C}$. The $d(001)$ standard errors are believed to be $\pm 0.2 \text{ \AA}$, and $P(\text{CO}_2)$ errors are at $\pm 1 \%$. Standard errors for pressure are not depicted.

For comparison with the experiments with $P(\text{CO}_2)$ increasing to ~ 500 bars, a series of experiments were made using He as the pressurizing gas (Table IV and Figure 4). In these experiments, the brine composition was 1.37 M and 3.42 M, the pressure ranged from 0 to 518 bars, and temperatures were from ~ 30 to 34°C . Because He is an inert gas that does not enter the interlayer of montmorillonite, but acts as a pressure medium, the similarity of both series of experiments to the CO_2 experiments indicates that at these conditions, CO_2 does not enter the interlayer of Na-SWy2.

Table IV. Helium pressure data.

M	$P(\text{He})$ (bar)	$T(^{\circ}\text{C})$	$d(001)$ (Å)	M	$P(\text{He})$ (bar)	$T(^{\circ}\text{C})$	$d(001)$ (Å)
1.37	0	29.6	19.0	3.42	0	30.4	15.8
	34.7	34.0	18.9		29.8	33.0	15.7
	60.0	34.5	18.8		55.3	33.8	15.7
	104.8	34.8	18.8		101.5	34.1	15.7
	212.7	34.9	18.8		221.7	34.2	15.6
	302.3	34.9	18.8		311.1	34.3	15.6
	412.3	34.9	18.8		404.2	34.3	15.6
	518.0	34.0	18.8		516.4	34.4	15.6

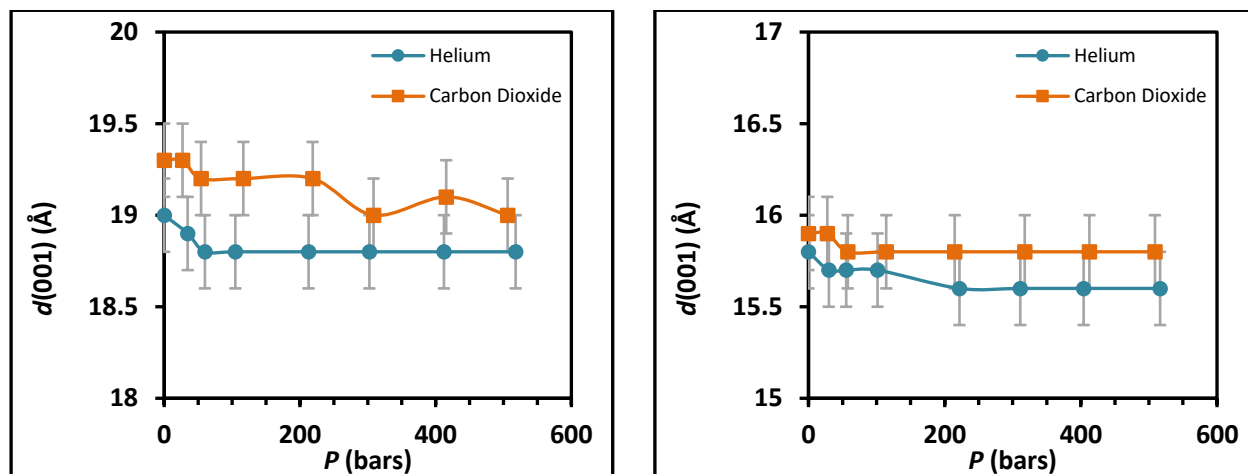


Figure 4. Effect of $P(\text{He})$ compared to the effect of $P(\text{CO}_2)$ on the $d(001)$ of montmorillonite at $T \sim 30$ to 34°C . Average He and CO_2 results using 1.37 M brine (left side) and 3.42 M brine (right side).

4.3 Experiments with initial $P(\text{CO}_2)$ and $P(\text{He})$ at ~500 bars and increasing T from ~31° to 150°C

Table V lists the results of experiments with eight brine compositions (0.17 M, 0.34 M, 0.68 M, 1.37 M, 1.71 M, 2.05 M, 3.42 M, >5.99 M). Figure 5 shows the effect of varying brine composition and temperature on the $d(001)$ of Na-SWy₂ at an initial $P(\text{CO}_2)$ of ~500 bars. In general, increasing temperature produces a decrease in $d(001)$, with the greatest effect at low to medium salinity. At temperatures of 75 to 100°C, major changes in $d(001)$ occur for selected salinity. For example, for the 1.71 M brine, the $d(001)$ decreased from 18.6 to 15.7 Å with increasing temperature. In Table V, two additional sets of experiments show similar changes in $d(001)$ in the presence of a 1.71 M brine (18.2 to 16.1 Å; 17.8 to 16.0 Å). In these experiments, the initial CO_2 pressures, at $T \sim 31^\circ\text{C}$, are 200.0 and 351.0 bars, as a function of temperature to ~150°C and ~125°C, respectively. The increase in pressure in the HPEC is shown as temperature increases. Standard errors associated with temperature are not given. For comparison, experiments using 1.37 M and 3.42 M brines with initial $P(\text{He})$ at ~515 bars and temperatures between 34 and 125 to 150°C (Table VI, Figure 6) show no significant difference between the $P(\text{CO}_2)$ and $P(\text{He})$ series of experiments.

Table V. Values of $d(001)$ for Na-SWy2 with $P(\text{CO}_2)$ variable as indicated and temperatures from ~30 to 150°C .

M	$P(\text{CO}_2)$ (bar)	T (°C)	$d(001)$ (Å)	M	$P(\text{CO}_2)$ (bar)	T (°C)	$d(001)$ (Å)
0.17 ^b	500	28.8	19.6	1.71 ^c	351.0	33.5	17.8
	620	50.0	19.5		384.4	50.0	17.5
	748	75.0	19.4		442.3	75.0	16.5
	876	100.0	19.3		506.0	100.0	16.1
	1004	125.0	19.1		573.1	125.0	16.0
	1132	150.0	19.0		635.5	150.0	16.0
0.34 ^b	500	29.1	19.9	1.71 ^b	500	33.6	18.6
	620	50.0	19.8		620	50.0	18.6
	748	75.0	19.8		748	75.0	18.1
	876	100.0	19.7		876	100.0	16.5
	1004	125.0	19.4		1004	125.0	15.8
	1132	150.0	19.2		1132	150.0	15.7
0.68 ^b	500	33.0	19.0	2.05 ^b	500	32.6	16.3
	620	50.0	19.2		620	50.0	16.0
	748	75.0	19.1		748	75.0	15.8
	876	100.0	19.0		876	100.0	15.7
	1004	125.0	19.0		1004	125.0	15.7
	1132	150.0	18.8		1132	150.0	15.7
1.37 ^{a,b}	500	33.2	19.0	3.42 ^{a,b}	500	33.1	15.8
	620	50.0	19.1		620	50.0	15.7
	748	75.0	19.0		748	75.0	15.8
	876	100.0	18.9		876	100.0	15.7
	1004	125.0	18.5		1004	125.0	15.8
	1132	150.0	17.2		1132	150.0	15.8
1.71 ^c	200.0	34.0	18.2	>5.99 ^b	500	33.0	15.5
	220.0	50.0	17.8		620	50.0	15.7
	254.0	74.9	16.7		748	75.0	15.6
	296.0	100.8	16.2		876	100.0	15.7
	337.0	124.1	16.2		1004	125.0	15.7
	361.0	132.0	16.1		1132	150.0	15.6

^a Values represent averaged data from two series. Errors in $d(001)$ values believed to be $\pm 2.5\%$

^b Pressures at the environmental chamber were not measured directly and were obtained by using Equation 1. Therefore, associated errors of pressure are high, near $\pm 10\%$.

^c Indicated CO_2 pressures were measured directly at the environmental chamber. The errors associated with these values are believed to be $\pm 1\%$.

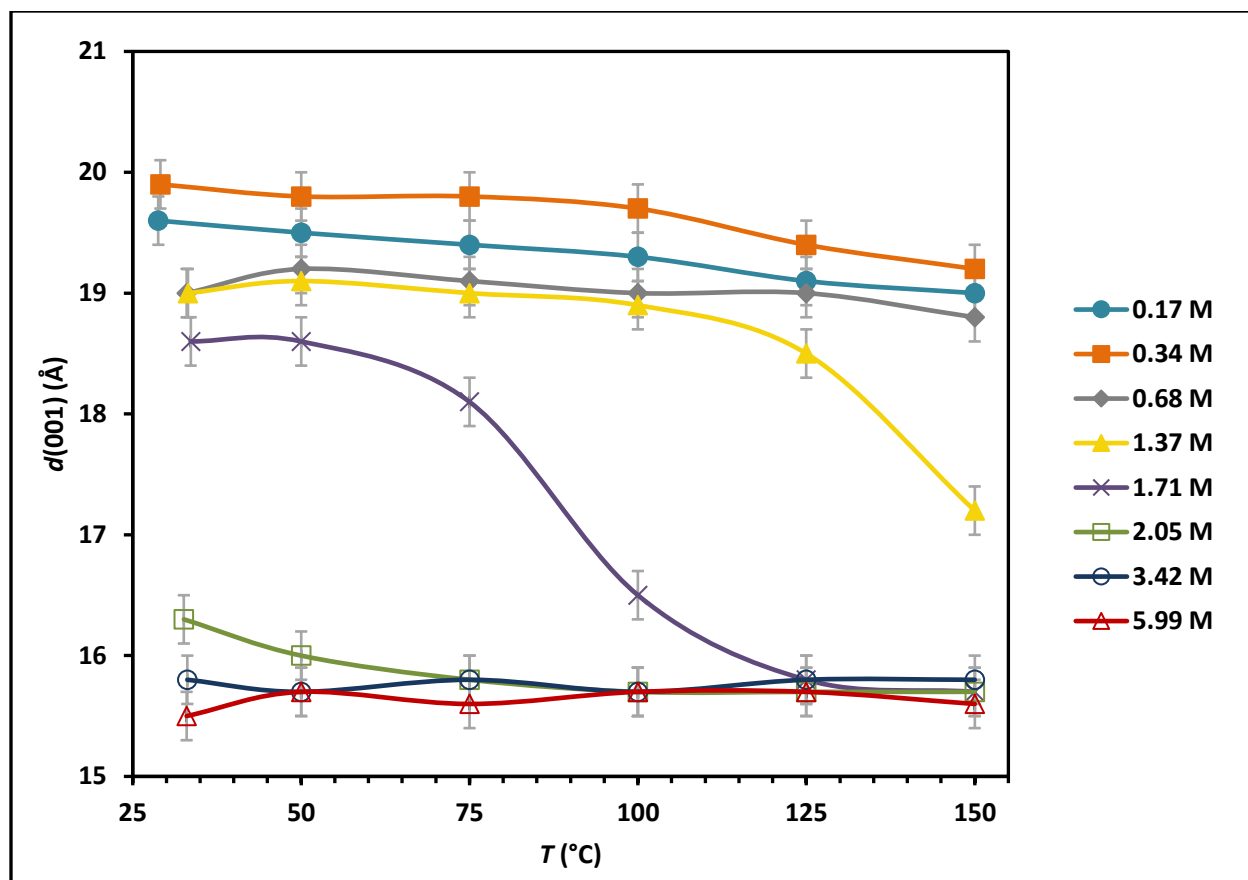


Figure 5. Effect of NaCl brine composition and temperature at $P(\text{CO}_2)$ starting at ~ 500 bars on the $d(001)$ of montmorillonite.

Table VI. Helium temperature data.

M	$P(\text{He})$ (bar)	T (°C)	$d(001)$ (Å)	M	$P(\text{He})$ (bar)	T (°C)	$d(001)$ (Å)
1.37	~ 517.5	34.0	18.8	3.42	~ 512.4	35.8	15.7
		50.0	18.7			50.0	15.7
		75.0	18.7			75.0	15.6
		100.0	18.5			100.0	15.6
		125.0	18.0			125.0	15.6
		150.0	16.8				

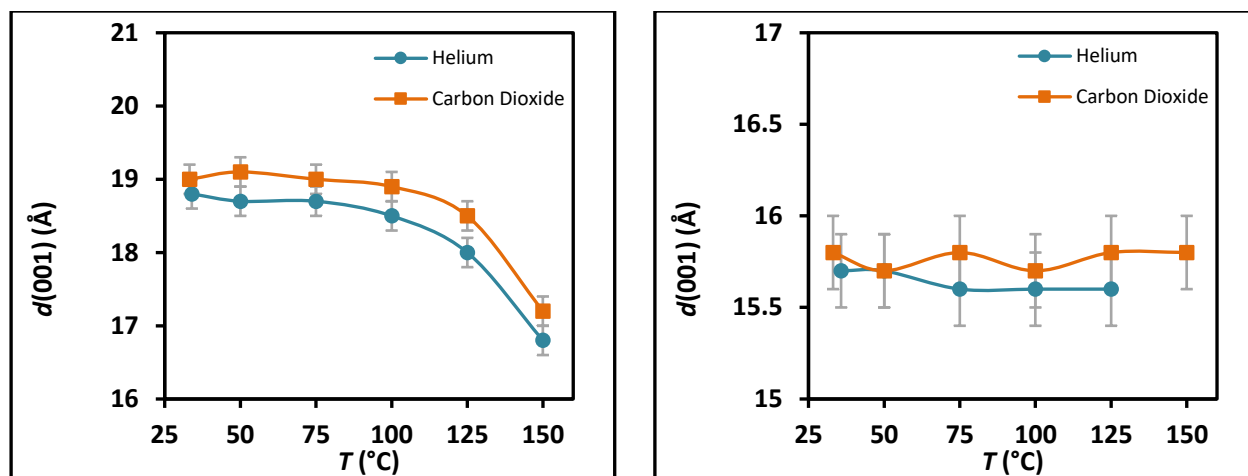


Figure 6. Comparison of the effect of temperature on the $d(001)$ of montmorillonite with $P(\text{He})$ and $P(\text{CO}_2)$ starting at ~ 500 bars. Average He and CO_2 results using 1.37 M brine (left side) and 3.42 M brine (right side).

5. DISCUSSION AND CONCLUSION

Rapid and sustained injection of vast quantities of CO₂ in sedimentary rocks is expected to sequester much of the CO₂-rich by-products of power stations, cement factories, and other industrial processes for long periods. Sandstone-shale sequences are of primary interest due to the high porosity and permeability of the sandstone reservoir, which is ideal for storing large volumes of CO₂, with the clay-rich, low permeability shale caprock preventing upward migration of CO₂. Clay minerals, such as smectites, are an important component in these formations, which are found as coatings on detrital grains in sandstone and an essential sealant in the confining shales. The ability of smectite clays to swell and contract is dependent on the activity of water, and can greatly impact the storage capacity of the sandstone reservoirs and sealing-capabilities of the shale caprocks.

The results of this study show that the interlayer H₂O content of the montmorillonite Na-SWy-2 is strongly dependent on the brine concentration, i.e., on the activity of water, which is temperature dependent. The effect of pressures greater than 500 bars is of secondary importance to temperature. The low temperature decrease in $d(001)$ from 18.9 Å to 16.6 Å at near ambient conditions (Table III) is a result of an increased brine solution concentration from 1.71 M to 2.05 M, respectively, and correlates to the stepwise expansion of the interlayer associated with intracrystalline swelling and the loss of interlayer H₂O. This loss of H₂O within the interlayer is primarily brine concentration controlled as the increase of pressure to ~500 bars resulted in minimal to no effect on the clay molar volume. In contrast, increasing the temperature resulted in significant dehydration of the interlayer for clay in the 1.71M brine at temperatures exceeding 50°C (18.6 Å to 15.7 Å, Table V). A similar decrease in $d(001)$ was observed for clay in the 1.37M brine solution when temperatures exceeded 100°C. Two (2) additional experiments were conducted using the 1.71 M brine with temperatures increasing stepwise from ~31° C to 150° C, but with varying initial starting pressures; the first series had an initial $P(\text{CO}_2)$ =200 bars and

the second series had an initial $P(\text{CO}_2)=351$ bars (Table V). A similar decrease in $d(001)$ was observed (17.8 Å to 16.1 Å and 17.8 Å to 16.0 Å, respectively), concluding that this significant decrease in clay molar volume is primarily brine concentration and temperature dependent, with negligible effects with increasing pressure.

A change in the molar volume of smectite in response to a change in $a(\text{H}_2\text{O})$ in the sedimentary reservoir rocks may have important implications for the long-term retention of the stored CO_2 . A large change in volume occurs where the interlayer distance goes from 19.0 Å to 17.2 Å (1.37 M brine) and 18.6 Å to 15.7 Å (1.71 M brine) with a temperature increase exceeding 100°C with a corresponding reduction in molar volume of Na-rich SWy2 by ~10 to 17%. This reduction in the clay particle volume has important implications on the sealing properties of the confining shales because this decrease in clay molar volume may lead to dehydration cracking, which would compromise the long-term sealing properties of the smectite containing, confining shales (Busch *et al.*, 2016).

Compared to a previous study (Colten, 1986) on $d(001)$ of a montmorillonite (SAz-1) at elevated pressure, the seven data points obtained in that study are consistent with the results presented here. However, Colten (1986, p. 388) suggested that an increase in pressure caused an increase in hydration, which is at variance with the results here for a more Na-rich smectite, although the differences in the smectite composition cannot be ruled out and those previous experiments involved $P(\text{H}_2\text{O})$ and not $P(\text{CO}_2)$. In contrast to the HPEC used in the present study, the cell used by Colten (1986) was limited to liquid-solid systems, where oriented clay aggregates are mounted on a flat substrate thus limiting contact of the sample with an applied liquid. Additionally, only higher 2θ values, i.e. for apparent $d(003)$ and $d(005)$ peaks, were monitored. Using pure H_2O at much greater pressures, Huang *et al.* (1994)

found that the “third hydration state” [$d(001) \sim 19 \text{ \AA}$] was stable up to 340°C and $P(\text{H}_2\text{O}) = 2 \text{ kbar}$ before dehydrating to a “second hydration state” [$d(001) \sim 16 \text{ \AA}$].

To determine the effect of CO_2 on the smectite structure, a limited set of experiments was performed using helium (He) as the pressure medium. Helium is an inert gas that is not expected to enter the interlayer of montmorillonite. The He experiments (Tables IV and VI; Figures 4 and 6) gave similar results (within two sigma) as the CO_2 experiments. Thus, pressure, temperature, and brine composition appear to be more important parameters than the choice of pressurizing gas (He or CO_2) in determining the swelling behavior, i.e. $d(001)$, of montmorillonite at similar hydration states [$a(\text{H}_2\text{O})$]. No evidence was found that CO_2 entered the interlayer of the smectite in any of the experiments under the water-saturated experimental conditions considered here.

The research presented here is considered exploratory and investigated the capabilities and limitations of the newly developed high-pressure environmental chamber (HPEC). Further research is recommended to address accurate measurements of pressure and pH within the HPEC during experiments. Additionally, research was limited to just one brine composition (NaCl) and one type of smectite clay (Na-montmorillonite SWy-2). For a more thorough understanding of the effects of CO_2 and $a(\text{H}_2\text{O})$ on smectite clays, further research should be conducted that includes varying brine compositions, as well as a variety of smectite clays. Benavides et al. (2020) begins to address some of these concerns by re-examining experimental parameters within the research presented here using a modified HPEC which allows for accurate pressure readings, as well as using a potassium exchanged montmorillonite (K-exchanged SWy-2).

REFERENCES

- Benavides, P.A., Kowalik, J., Guggenheim, S., Koster van Groos, A.F., 2020. Effect of CO₂ pressure, temperature, and brine composition on the interlayer spacing of Na-Rich and K-exchanged montmorillonite. *Applied Clay Science* 198.
- Busch, A.; Bertier, P.; Gensterblum, Y.; Rother, G.; Spiers, C. J.; Zhang, M.; Wentinck, H. M. On sorption and swelling of CO₂ in clays. *Geomech. Geophys. Geo-Energy Geo-Res* **2016**, 2(2), 111-130. DOI: 10.1007/s40948-016-0024-4
- Colten, V. A., 1986. Hydration states of smectite in NaCl brines at elevated pressures and temperatures. *Clays and Clay Minerals* 34, 385-389.
- Costanzo, P.M., Guggenheim, S., Eds. 2001. Baseline studies of the Clay Minerals Society Source Clays, *Clays and Clay Minerals* 49 (5).
- Espinoza, D. N., Santamarina, J.C., 2012. Clay interaction with liquid and supercritical CO₂: The relevance of electrical and capillary forces. *International Journal of Greenhouse Gas Control* 10, 351–362.
- Giesting, P., Guggenheim, S., Koster van Groos, A.F., Busch, A., 2012a. Interaction of carbon dioxide with Na-exchanged montmorillonite at pressures to 640 bars: Implications for CO₂ sequestration. *International Journal of Greenhouse Gas Control* 8, 73–81.
- Giesting, P., Guggenheim, S., Koster van Groos, A.F., Busch, A., 2012b. X-ray diffraction study of K- and Ca-exchanged montmorillonite in CO₂ atmospheres. *Environmental Science & Technology* 46, 5623-5630.
- Guggenheim, S., Koster van Groos, A. F., 2014. An integrated experimental system for solid-gas-liquid environmental cells. *Clays and Clay Minerals* 62, 479-485.
- Huang, W-L., Bassett, W.A., Wu, T-C., 1994. Dehydration and hydration of montmorillonite at elevated temperatures and pressures monitored using synchrotron radiation. *American Mineralogist* 79, 683-691.
- IPCC (Intergovernmental Panel on Climate Change), 2005. IPCC Special report on carbon dioxide capture and storage. Working Group III, Metz, B., Davidson, O., de Coninck, H., Loos, M., Meyer, L.A., eds., Cambridge University Press, United Kingdom, 442 pp.
- Kowalik, J., Guggenheim, S., Koster van Groos, A.F. (2015, July 5-10). Effects of temperature, pressure, and brine composition on the interlayer spacing of montmorillonite at *in situ* conditions using CO₂. Euroclay 2015, Edinburgh, Scotland.
- Lin, H., Fujii, T., Takisawa, T., Takahashi, T., Hasida, T., 2008, Experimental evaluation of interactions in supercritical CO₂/water/rock minerals system under geologic CO₂ sequestration conditions. *Journal of Material Science* 43, 2307-2315.

- Loring, J.S., Schaef, H.T., Thompson, C.J., Turcu, R.V., Miller, Q.R., Chen, J., Hu, J., Hoyt, D.W., Martin, P.F., Ilton, E.S., Felmy, A.R., and Rosso, K.M., 2013. Clay hydration/dehydration in dry to water-saturated supercritical CO₂: Implications for caprock integrity. *Energy Procedia* 37, 5443-5448.
- Makaremi, M., Jordan, K. D., Guthrie, G. D., Myshakin, E. M., 2015. Multiphase Monte Carlo and Molecular Dynamics Simulations of Water and CO₂ Intercalation in Montmorillonite and Beidellite. *Journal of Physical Chemistry C* 119, 15112-15124.
- Michael, K., Golab, A., Shulakova, V., Ennis-King, J., Allinson, G., Sharma, S., Aiken, T., 2010. Geological storage of CO₂ in saline aquifers – A review of the experience from existing storage operations. *International Journal of Greenhouse Gas Control* 4, 659-667.
- Michels, L., Fossum, J. O., Rozynek, Z., Hemmen, H., Rustenberg, K., Sobas, P. A., Kalantzoulou, G. N., Knudsen, K. D., Janek, M., Plivelic, T. S., da Silva, G. J., 2015. Intercalation and retention of carbon dioxide in a smectite clay promoted by interlayer cations. *Scientific Reports* 5, 8775.
- Morsy, S., Sheng, J.J., 2014. Effect of water salinity on shale reservoir productivity. *Advances in Petroleum Exploration and Development* 8, 9-14.
- Norrish, K., 1954. Swelling of montmorillonite. *Discussions of the Faraday Society* 18, 120-134.
- Norrish, K., Quirk, J.P., 1954. Crystalline swelling of montmorillonite. *Nature* 173, 255-256.
- Omekeh, A. V., Evje, S., Friis, H.A., 2004. Modeling of low salinity effects in sandstone oil rocks. *International Journal of Numerical Analysis and Modeling* 1, 1-18.
- Schaef, H.T., Loring, J.S., Glezakou, V-A., Miller, Q.R.S., Chen, J., Owen, A.T., Lee, M-L., Ilton, E.S., Felmy, A.R., McGrail, B.P., Thompson, C.J., 2015. Competitive sorption of CO₂ and H₂O in 2:1 layer phyllosilicates. *Geochimica Cosmochimica Acta* 161, 248-257.
- Sena, M.M., Morrow, C.P., Kirkpatrick, R.J., Krishnan, M., 2015. Supercritical carbon dioxide at smectite-water interfaces: Molecular dynamics and adaptive biasing force investigation of CO₂/H₂O mixtures nanoconfined in Na-montmorillonite. *Chemical Materials* 27, 6946-6959.
- Slade, P.G., Quirk, J.P., Norrish, K., 1991. Crystalline swelling of smectite samples in concentrated NaCl solutions in relation to layer charge. *Clays and Clay Minerals* 39, 234-238.
- Underwood, T., Erastova, V., Cubillas, P., Greenwell, H.C., 2015. Molecular dynamic simulations of montmorillonite-organic interactions under varying salinity: An insight into enhanced oil recovery. *Journal of Physical Chemistry C* 119, 7282-7294.
- Wu, T-C., Bassett, W.A., Huang, W-L., Guggenheim, S., Koster van Groos, A.F., 1997. Montmorillonite under high H₂O pressures: stability of hydrate phases, rehydration hysteresis, and the effect of interlayer cations. *American Mineralogist* 82, 69-78.

- Xu, T., Apps, J.A., Pruess, K., 2003. Reactive geochemical transport simulation to study mineral trapping for CO₂ disposal in deep arenaceous formations. *Journal of Geophysical Research* 108 (B2).
- Xu, Y., Xiang, G., Jiang, H., Chen, T., Chu, F., 2014. Role of osmotic suction in volume change of clays in salt solution. *Applied Clay Science* 101, 354-361.

APPENDIX



Dear Jacqueline Kowalik,

Thank you for your query.

Please note that, as one of the authors of this article, you retain the right to reuse it in your thesis/dissertation. You do not require formal permission to do so. You are permitted to post this Elsevier article online if it is embedded within your thesis. You are also permitted to post your Author Accepted Manuscript online.

However posting of the final published article is prohibited.

*"As per our [Sharing Policy](#), authors are permitted to post the Accepted version of their article on their institutional repository – as long as it is for **internal institutional use only**.*

It can only be shared publicly on that site once the journal-specific embargo period has lapsed. For a list of embargo periods please see: [Embargo List](#).

You are not permitted to post the Published Journal Article (PJA) on the repository."

Please feel free to contact me if you have any queries.

Regards,

Kaveri

Permissions Helpdesk
ELSEVIER | Operations

VITA

NAME: Jacqueline Kowalik

EDUCATION: B.S., Geoscience, Winona State University, Winona, Minnesota, 2008

TEACHING: Department of Earth and Environmental Sciences, University of Illinois at Chicago, Chicago, Illinois;
Earth and Environmental Science 111, Earth Materials, Mineralogy and Field Trip in Missouri

RESEARCH: Department of Earth and Environmental Sciences, University of Illinois at Chicago, Chicago, Illinois
Clay Mineralogy and X-Ray Diffraction Laboratories

ABSTRACTS: Kowalik, J., Guggenheim, S., Koster van Groos, A.F. (2015, July 5-10). Effects of temperature, pressure, and brine composition on the interlayer spacing of montmorillonite at in situ conditions using CO₂. Euroclay 2015, Edinburgh, Scotland.

PUBLICATIONS: Benavides, P.A., Kowalik, J., Guggenheim, S., Koster van Groos, A.F., 2020. Effect of CO₂ pressure, temperature, and brine composition on the interlayer spacing of Na-Rich and K-exchanged montmorillonite. Applied Clay Science 198.